

Identification of Curcumin Targets in the Brain of Epileptic Mice Using DARTS

Ninan Zhang,[#] Ruifan Lin,[#] Honglin Xu, Xianghong Jing, Hongwei Zhou, Xiaoxiao Wen, and Qi Xie*

Cite This: *ACS Omega* 2024, 9, 22754–22763

Read Online

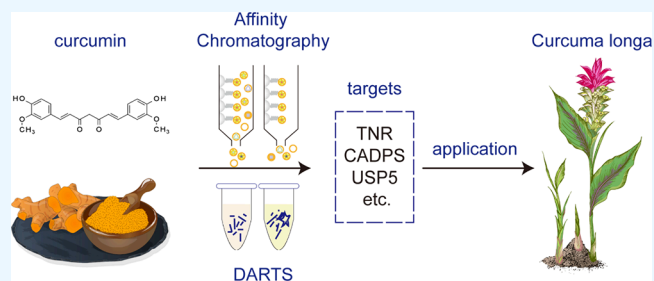
ACCESS |

Metrics & More

Article Recommendations

Supporting Information

ABSTRACT: Curcumin, a compound derived from turmeric, is traditionally utilized in East Asian medicine for treating various health conditions, including epilepsy. Despite its involvement in numerous cellular signaling pathways, the specific mechanisms and targets of curcumin in epilepsy treatment have remained unclear. Our study focused on identifying the primary targets and functional pathways of curcumin in the brains of epileptic mice. Using drug affinity responsive target stabilization (DARTS) and affinity chromatography, we identified key targets in the mouse brain, revealing 232 and 70 potential curcumin targets, respectively. Bioinformatics analysis revealed a strong association of these proteins with focal adhesions and cytoskeletal components. Further experiments using DARTS, along with immunofluorescence staining and cell migration assays, confirmed curcumin's ability to regulate the dynamics of focal adhesions and influence cell migration. This study not only advances our understanding of curcumin's role in epilepsy treatment but also serves as a model for identifying therapeutic targets in neurological disorders.



INTRODUCTION

Epilepsy is a major health concern, affecting an estimated 70 million individuals globally and ranking as one of the most common neurological disorders. The condition's intricate pathophysiology often necessitates long-term pharmacological management.¹ Despite well-established protocols for the administration of antiepileptic drugs (AEDs), significant challenges remain. Notably, 20–30% of patients experience inadequate responses to existing medications. Additionally, the potential for drug–drug interactions, adverse effects, and teratogenic risks associated with AEDs adds layers of complexity to patient care.^{2,3} These persistent issues highlight the critical demand for the development of new antiepileptic medications that are both safe and effective.

Curcumin, a plant polyphenol derived from the rhizomes of ginger family plants such as *Curcuma longa*,⁴ has been confirmed to have potential efficacy and safety in the treatment of epilepsy through multiple clinical studies.^{5–7} Notably, curcumin therapy does not interfere with the absorption, digestion, metabolism, or excretion of other antiepileptic drugs (such as sodium valproate, phenytoin, phenobarbital, and carbamazepine), and it can enhance their therapeutic effects while reducing the dosage and side effects.⁸ Currently, genomics-based drug repurposing techniques have identified curcumin as one of the most promising natural candidates for antiepileptic medication.⁹ However, there are still challenges regarding the unclear molecular mechanism of curcumin, as well as its poor bioavailability and instability.⁴ In particular, the unknown molecular mechanism of action of curcumin poses

obstacles for optimizing its molecular structure toward improved therapeutic potential.

DARTS is a useful method for identifying natural drug targets. This is due to its ability to maintain drugs in their native state, which ensures that they interact authentically with target proteins. One of the advantages of DARTS is that it does not require prior knowledge of the drug's activity.¹⁰ This makes it an ideal tool for exploring unknown mechanisms of natural compounds. The method is compatible with complex biological mixtures and offers an unbiased approach to detect both expected and unexpected targets, including off-target effects.

Research has indicated that curcumin exhibits therapeutic and preventive effects on acute and chronic epilepsy models in mice, involving processes such as antioxidation, neuroprotection, and anti-inflammation.¹¹ Nevertheless, current studies still lack precise identification of the key targets directly affected by curcumin. Curcumin has multiple targets and participates in various cellular signaling pathways, but exactly which pathways regulate critical signals in epilepsy have not yet been reported. This study aims to investigate the key

Received: January 25, 2024

Revised: April 28, 2024

Accepted: May 9, 2024

Published: May 16, 2024



pathways and targets of curcumin in treating epilepsy through DARTS combined with affinity chromatography.

MATERIALS AND METHODS

Materials and Reagents. The following were used in the study: epoxy-activated Sepharose 6B (Sigma-Aldrich, E6754) and Sepharose 6B (Sigma-Aldrich, 6B100), curcumin (Solarbio, C7090), recombinant human pleiotrophin (RayBio, 230-00618), pilocarpine (Cayman, 14487), scopolamine (Macklin, 6106-46-3), diazepam (Sigma-Aldrich, 439-14-5), Dulbecco's modified Eagle's medium/Ham's F-12 (WISSENT, 219-001-LL), fetal bovine serum (VivaCell, C04001-050), P/S (Pricella, PB180120), bovine serum albumin (AMRESCO, 9048-46-8), Tris (Solarbio, T8060), NaCl (SCR, 7647-14-5), glycine (VWR, 56-40-6), glycerol (Sigma-Aldrich, 1040950250), dithiothreitol (Sigma-Aldrich, 20-265), Complete Protease Inhibitor Cocktail (Roche, CO-RO), phosphatase inhibitor cocktail (Sigma-Aldrich, 524633), dimethyl sulfoxide (Solarbio, D8371), sodium thiosulfate (Aladdin, 7772-98-7), sodium dodecyl sulfate (Macklin, S817789), bromoxylene blue (Macklin, B871865), 2-hydroxy-1-ethanethiol (Sigma-Aldrich, 60-24-2), Brilliant Blue R (Macklin, B802269), methyl alcohol (Sigma-Aldrich, 67-56-1), acetic acid (SCR, 64-19-7), acrylamide (SCR, 79-06-1), ammonium persulfate (SCR, 7727-54-0), tetramethylethylenediamine (SCR, 110-18-9), nonfat dry milk (Beyotime, P0216), silver nitrate (SCR, 7761-88-8), Na₂CO₃ (SCR, 497-19-8), NaOH (SCR, 1310-73-2), dimethylformamide (Sigma-Aldrich, 68-12-2), tribromethanol (Aladdin, 75-80-9), Hepes (SCR, C21500), ethylenediaminetetraacetic acid (SCR, 60-00-4), phenylmethanesulfonyl fluoride (Sigma-Aldrich, 329-98-6), CH₃COOK (SCR, 127-08-2), MgSO₄ (SCR, 7487-88-9), KCl (SCR, 7447-40-7), Na₂HPO₄ (SCR, 7558-79-4), KH₂PO₄ (SCR, 7778-77-0), HCl (SCR, 7647-01-0), Tween-20 (Solarbio, T8220), trehalose (Sigma-Aldrich, 64622-92-0), paraformaldehyde (SCR, 30525-89-4), Triton-X-100 (Aladdin, T109026), pronase E (Roche, 11459643001), bovine serum albumin (AMRESCO, 9048-46-8), Amicon (Millipore, UFC5003), anti-FAK antibody (BD, 1:200, 610087), anti- α -tubulin antibody (Sigma-Aldrich, T9026, 1:10000), goat HRP-conjugated antimouse IgG (CWBIO, CW0102S, WB 1:1000), Alexa Fluor 488 phalloidin (Invitrogen, IF 1:500, A12379), and goat Alexa Fluor 555-conjugated antirabbit (Invitrogen; IF 1:500, A27039).

Animals. Male ICR mice, weighing 30 ± 2 g, were obtained from Beijing Vital River Experimental Animal Technology Co., Ltd. All mice were housed and cared for following the guidelines of the Experimental Animal Center at the Institute of Genetics and Developmental Biology, Chinese Academy of Sciences. The mice were maintained under specific pathogen-free conditions in the animal facility and were kept on a 12 h light/12 h dark cycle with ad libitum access to food and water.

Cell Culture. The cell line U251 was cultured in a mixture of Dulbecco's modified Eagle's medium/Ham's F-12 in a 1:1 ratio with 10% fetal bovine serum and 1% P/S at 37 °C in 5% CO₂.

Pilocarpine Epilepsy Model. The pilocarpine epilepsy model was developed by the Turski group.^{12,13} In our experiments, adult male ICR mice were intraperitoneally injected with pilocarpine (290 mg/kg, ig) preceded by the administration of scopolamine (1.5 mg/kg) 30 min before. After pilocarpine injection, mice exhibiting status epilepticus (SE) lasting for more than 120 min were selected, and

diazepam (10 mg/kg) was administered to terminate the seizures. The progression of seizures resembled the classification observed in the kindling model by Racine.¹⁴ Brains were dissected on the fourth day post-SE for further study.

Identification of Target Proteins by DARTS with Mass Spectrometry. DARTS based on the work of Pai et al.,¹⁰ was used to identify curcumin targets. Three mice were employed for DARTS. Brain lysate derived from mice was subjected to the pilocarpine procedure containing 50 mM Tris-HCl (pH 7.4), 200 mM NaCl, 10% glycerol, 2 mM dithiothreitol (DTT), 1% Complete Protease Inhibitor Cocktail (PIC), and 1% phosphatase inhibitor cocktail, homogenize for 2 min at 4 °C according to the ratio of 1 mg brain tissue to 10 μ L lysis buffer, and fully decomposed at 4 °C. The fractured brain tissue was centrifuged at 4 °C and 150,000g for 30 min. We measured protein concentration using the BCA method and diluted the supernatant to 7 mg/mL using the brain lysis buffer. We took two parts of 99 μ L supernatant respectively treated with 1 μ L 2 mg/mL curcumin or 1 μ L dimethyl sulfoxide (DMSO) as a control in 37 °C for 30 min. And each sample was divided into 20 μ L aliquots, and 2 μ L pronase E was added according to concentrations of about 1:1000, 1:10,000, and 1:200,00. We also performed experiments with digestion times of 5, 10, and 15 min. An undigested sample (UD) instead received ultrapure water. All samples were incubated at room temperature for 15 min. To stop the digestion reaction, 2 μ L of 20 \times PIC was added followed by a 10 min incubation on ice. Subsequently, 6 \times sample buffer was added to achieve a final concentration of 1 \times containing 50 mM Tris-HCl (pH 6.8), 100 mM DTT, 2% (w/v) sodium dodecyl sulfate (SDS), 0.1% (w/v) bromoxylene blue, and 10% (v/v) glycerol, and the samples were heated at 95 °C for 5 min. Subsequently, the samples were separated by 10% SDS-PAGE, and Coomassie Brilliant Blue (CBB) staining was used to identify protein bands that are protected from curcumin. The target bands were cut for mass spectrum analysis (Figure 2b).

Identification of Target Proteins by Affinity Chromatography and Mass Spectrometry. *Establishment of Stationary Phases for Coupling Curcumin to Epoxy Activated Sepharose 6B (EAS6B).* One gram of EAS6B was washed in 50 mL of cold distilled water through five cycles, with each cycle involving centrifugation at 1500g for 5 min, yielding approximately 3.5 mL of swollen EAS6B, which was collected in 20% ethanol and stored at 4 °C for later use. Curcumin was dissolved in coupling buffer containing 100 mM Na₂CO₃, 10 mM NaOH, and 50% dimethylformamide to a final concentration of 20 mM. Two volumes of the coupling reagent were mixed with 1 vol of swollen beads and shaken overnight in the dark at 30 °C. On the following day, the sepharose-curcumin suspension was washed three times with the coupling buffer and incubated overnight at 30 °C with 1 M glycine to block any remaining nonspecific binding sites. Uncoupled beads were prepared by incubating EAS6B with 1 M glycine. Uncoupled beads and curcumin-coupled beads were packed into a chromatography column, and subsequent washing steps were carried out according to the manufacturer's instructions.

Mouse Brain Whole Protein Extraction. We took three mice to complete affinity chromatography. Mouse abdominal injection of tribromoethanol (20 μ L/g) was used for anesthesia. The brain was isolated by cardiac perfusion with ice-cold saline solution removed from the skull, and the brainstem was dissected out. The brain was then rinsed with an

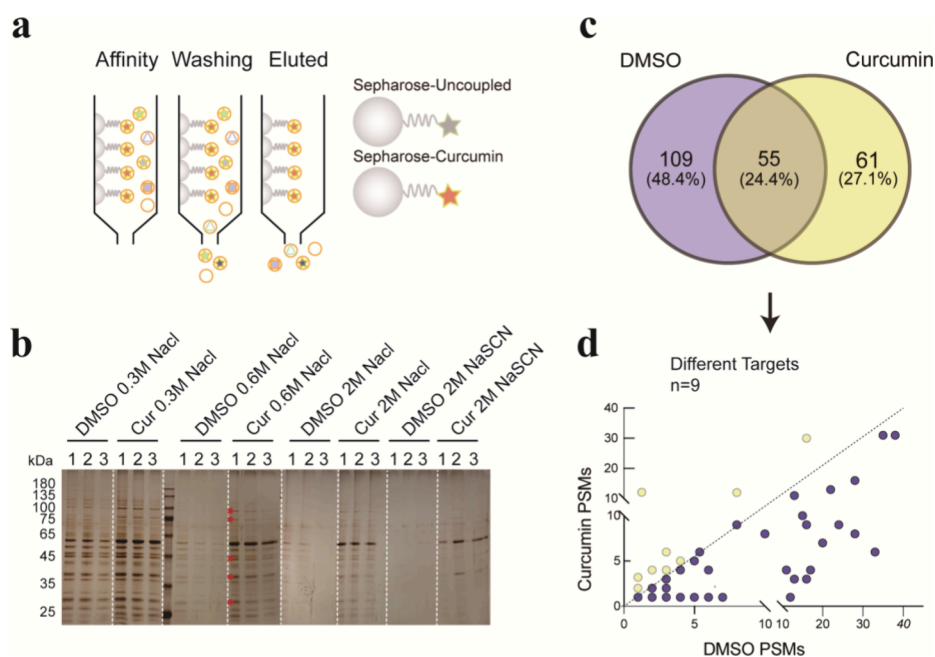


Figure 1. Identification of curcumin target proteins in the brain of epileptic mice using affinity chromatography and mass spectrometry. (a) Schematic diagram illustrating the affinity chromatography method used with sephacrose-uncoupled in the negative condition and sephacrose-curcumin in the experimental condition. (b) Silver stained SDS-PAGE gels showing proteins eluted from affinity columns using increasing concentrations of NaCl or NaSCN, with red stars indicating differential protein bands that appear to be unique to or enhanced in the sephacrose-curcumin condition. 1, 2, and 3 indicate sequential samples of eluate collected at a 10% SDS-PAGE. (c) The Venn diagram shows two groups of mass spectrometry data profiles derived from control or curcumin conditions. Among them, 61 proteins marked in yellow are the specific combined proteins of curcumin. (d) Scatter plot of 55 differential proteins. Among them, the PSM value of the nine proteins marked yellow above the dashed line were 1.5 times higher than the DMSO group.

ice-cold saline solution. A lysis buffer consisting of 50 mM Hepes buffer (pH 7.45), 50 mM NaCl, 1 mM ethylenediaminetetraacetic acid (EDTA), 2 mM DTT, 1 mM phenylmethanesulfonyl fluoride (PMSF), and 1% PIC was added in a volume ratio of 1:4. Tissue homogenization was performed using both a tissue disruptor and a glass homogenizer. The homogenate was precooled and centrifuged at 600g for 20 min to remove the pellet followed by a 4 °C ultracentrifugation at 15,000g for 60 min to obtain the supernatant.

Desalination and Decontextualization of Soluble Protein Extracts. The desalting buffer contained 20 mM Hepes (pH 7.45), 150 mM CH_3COOK , 1 mM EDTA, 1 mM PMSF, 2 mM DTT, and 5 mM MgSO_4 . Protein samples were diluted 1000 folds and then concentrated using 3 kDa ultrafiltration tubes. After desalting, the samples were supplemented with 100 mM trehalose, 0.1% glycine, and 1% PIC and stored on ice. A desalting column was prepared, filled with 10 mL of Sepharose 6B, washed with five column volumes of ultrapure cold water, and then equilibrated with three column volumes of desalting buffer. The desalted samples were passed through the desalting column to remove nonspecific binding sites. The column was washed with the desalting buffer, the eluted solution was collected, and its protein concentration was checked using the Bradford assay. The flow-through was concentrated to 800 μL using 3 kDa ultrafiltration tubes supplemented with 100 mM trehalose, 0.1% glycine, and 1% PIC, and the final protein concentration was determined using the bicinchoninic acid (BCA) assay. Finally, the samples were divided into two portions and stored on ice for later use.

Elution of Protein from Affinity Column from Stationary Phases. The chromatography column was equilibrated with a

volume of desalting buffer five times the column volume. After the liquid flow had finished, the final desalted and concentrated protein sample was applied to the column. The column was then washed with a volume of desalting buffer eight times the column volume, and washing was stopped when no protein in the flow-through was detected by the Bradford assay. Bound proteins were eluted using gradients of 0.3 M NaCl, 0.6 M NaCl, 2 M NaCl, and 2 M NaHS, each with a volume of two times the column volume. Then, 10% SDS was added to the eluate to achieve a final concentration of 1%, and the mixture was boiled at 95 °C for 5 min. Ten microliter samples were subjected to 10% SDS-PAGE followed by silver staining to assess whether the proteins are protected by curcumin, and mass spectrometry of remaining eluted proteins was conducted.

Biological Information Analysis. To screen target proteins identified by mass spectrometry, KEGG pathway and molecular function analyses were conducted using the Metascape database (<http://metascape.org/>). Venn diagrams were created using a tool available online (<https://bioinfogp.cnb.csic.es/tools/venny/index.html>). When $P < 0.01$, the minimum number of annotated genes was three as the condition for screening.

Immunofluorescence Staining. Coverslips were coated with 150 nM pleiotrophin (PTN) at 37 °C for 120 min followed by three washes with 1 \times PBS containing 13.7 mM NaCl, 0.27 mM KCl, 0.8 mM Na_2HPO_4 , and 0.2 mM KH_2PO_4 . Then, these slides that have been covered by PTN were coated with 100 μM curcumin at 37 °C for 120 min and again washed three times with 1 \times PBS for the experimental group. U251 cells were fixed with 2.5% paraformaldehyde (PFA) at 37 °C for 10 min after growing for 50 min followed

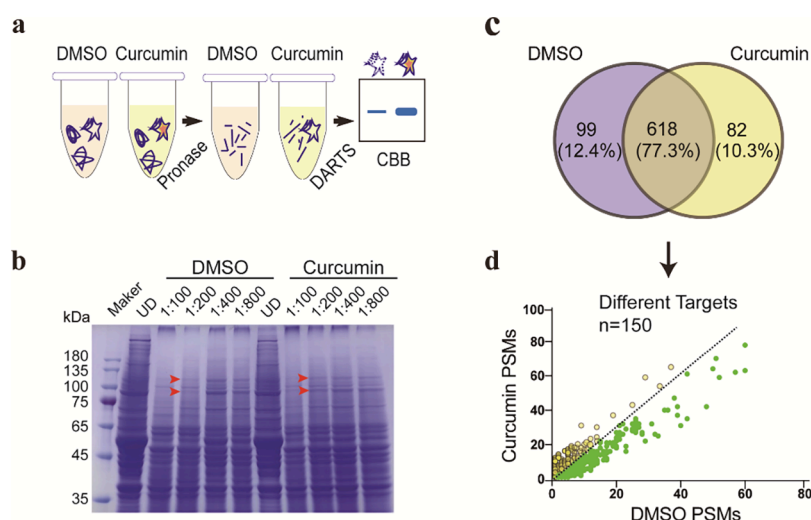


Figure 2. Identification of curcumin target proteins in the brain of epileptic mice by DARTS combined with mass spectrometry. (a) Schematic diagram depicting the DARTS method for uncovering curcumin target proteins. (b) Red arrows indicate differential bands with increased intensity in the presence of curcumin relative to the negative control (DMSO), to detect the composition of the difference bands, then these strips excised from 10% SDS-PAGE gels and subjected to mass spectrometry. These two bands show intensity differences at 1:200 ratios. As the concentration of pronase E decreases, this difference gradually diminishes. (c) A Venn diagram showing two groups of mass spectrometry data profiles. Among them, 82 proteins marked in yellow are the specific combined proteins of curcumin. (d) Scatter plot of PSMs of shared protein. Among them, the PSM values of the 150 proteins marked yellow above the dashed line were 1.5 times higher than the DMSO group.

by three washes with 1× PBS. Cells were permeabilized and blocked with 3% bovine serum albumin (BSA) and 0.1% Triton-X-100 in PBS for 30 min. The primary antibody against focal adhesion kinase (FAK) was diluted in a blocking buffer and incubated at room temperature for 1.5 h. After three washes with PBS containing 0.1% Triton-X-100 (PBST), the secondary antibody was applied at room temperature for 1.5 h followed by three washes with PBST. Imaging was performed using a Zeiss Observer Z1 microscope. The cell area and area of FAK signals were measured using Fiji/ImageJ. Student's *t* test was used for continuous data analysis in GraphPad Prism. Error bars represent mean \pm SD.

Wound Healing Assay. U251 cells were plated in six-well plates at a density of 1.5×10^5 per well. Cells were cultured overnight until they were fully attached to the wall. The top row of three wells was given a concentration of 100 nM PTN, and the lower row of three wells was given a concentration of 100 nM PTN and 10 μ M curcumin. Then, a straight scratch was made using a white tip to stimulate the wound, and a digital image of the marked wound area was taken at 9 h intervals. Cell numbers were counted each time the wound areas were captured.

Verification by DARTS Results Using Western Blotting. U251 cells were lysed using a buffer consisting of 10 mM Tris-HCl (pH 7.4), 200 mM NaCl, 10% glycerin, 2 mM DTT, 1% PIC, and 1% phosphate inhibitor. The lysate was centrifuged at 10,000g for 20 min (4 °C), and the protein concentration of the obtained supernatant was determined by the BCA assay. An aliquot of 99 μ L of the lysate was split into two 1.5 mL tubes treated with 2 mg/mL curcumin or DMSO as the control for 30 min in a constant temperature shaker at 28 °C. Each sample was split into 20 μ L samples, and 2 μ L 1% (w/w) of pronase E was added sequentially, or the same volume of ultrapure water was added to the UD, and then all samples were incubated for 15 min at room temperature. Each digestion reaction was stopped by adding 2 μ L of 20× PIC and incubated on ice for 10 min. The 6× sample buffer was added

to make the final concentration 2×, and the samples were heated at 95 °C for 5 min. Finally, each sample was analyzed using SDS-PAGE and Western blotting. Individual bands were normalized with α -tubulin as a reference. Normalized values were analyzed using GraphPad Prism.

Statistical Analysis. The data were analyzed by GraphPad Prism 8.0 software and are presented as the mean \pm SEM. The statistics were analyzed by using an unpaired *t* test for two groups and multiple *t* tests for multiple groups. **P* < 0.05, ***P* < 0.01, ****P* < 0.001, and *****P* < 0.0001 were considered statistically significant.

RESULTS

Acquisition and Screening of Candidate Targets of Curcumin in the Brain of Epileptic Mice. To identify the target proteins of curcumin in the brain of epileptic mice, we initially divided samples of brain extract from pilocarpine-treated mice into equal portions and loaded them onto either a sepharose-curcumin affinity column or an uncoupled column (Figure 1a). Extract proteins bound to the columns were then eluted in three sequential fractions. Analysis of these fractions by SDS-PAGE followed by silver staining showed significant differences from the two columns (Figure 1b).

Based on this, we selected the samples eluted with 0.6 M NaCl for further mass spectrometry analysis (Figure 1b). The results identified 164 proteins in the control and 116 proteins in the curcumin condition, with 55 proteins shared between the two groups and 61 proteins unique to the curcumin coupled group (Figure 1c). We also plotted the peptide-to-spectrum matches (PSMs) values of the 55 proteins shared in both groups and found a small subset of 9 proteins with PSM values greater than 1.5 times that of the control group, indicating that these 9 proteins accumulate to a higher level in the curcumin-coupled condition. Taken together, our affinity chromatography approach yielded 70 potential protein targets of curcumin (61 binding proteins specific to the curcumin group were labeled yellow in Figure 1c, and 9 binding proteins

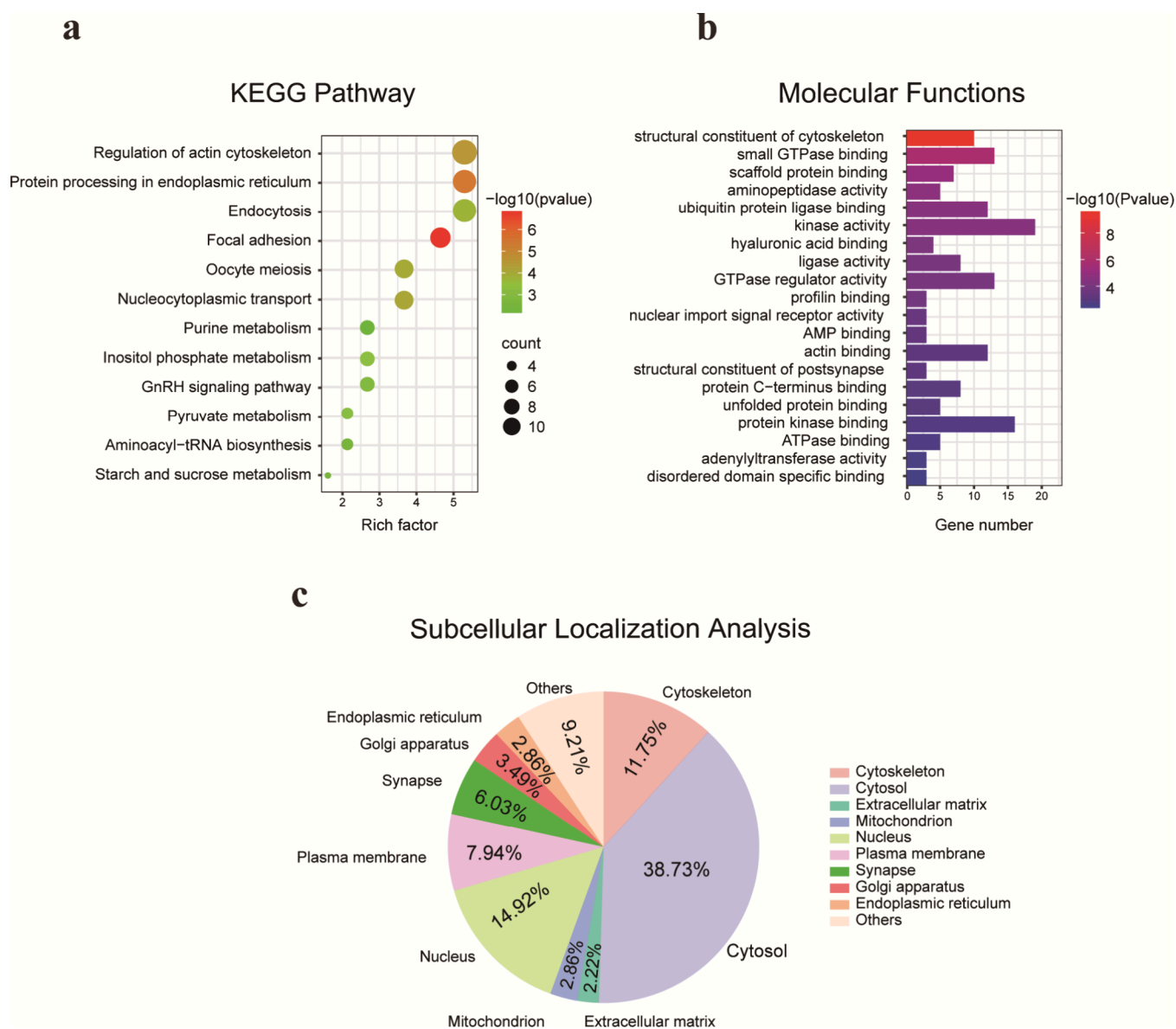


Figure 3. Analysis of protein targets identified in our screens. (a) Bubble plots representing the KEGG analysis. Colors indicate the P value, and the size of the bubbles represents the number of enriched pathways. (b) GO-MF (Gene Ontology molecular functions analysis). Colors represent the P value. (c) Subcellular localization analysis of curcumin targets.

in the curcumin group whose PSM value was higher than that of the DMSO group were labeled yellow above the dashed line in Figure 1d).

Considering the limitations of affinity chromatography for chemically modified small molecules, we sought to obtain more authentic and reliable data while reducing experimental system induced errors. We therefore conducted experiments using DARTS to further explore curcumin targets. The DARTS approach relies on the principle that target proteins bound to small molecules like curcumin are resistant to proteolytic cleavage. This technique has the unique advantage that it does not require any immobilization or structural modifications of the small molecule being studied (Figure 2a). This method is a relatively fast and direct approach for identifying potential protein targets of a small molecule.¹⁰ We used brain extracts from three epileptic mice in the DARTS assay to identify target proteins that are resistant to protease in the presence of curcumin. CBB staining after SDS-PAGE

showed band intensity differences between DMSO and the curcumin-treated samples that were incubated with pronase E/protein concentrations of 1:100 and 1:200. We chose samples treated with pronase E/protein concentrations ratio of 1:200 for further analysis by mass spectrometry (Figure 2b). At the same time, we also set the digestion time to 5, 10 and 15 min for the DARTS experiment (Figure S1). Proteomic analysis identified 717 proteins in the DMSO-treated sample and 700 proteins in the curcumin-treated sample, 82 of which were specific to the curcumin treated group and the remaining 618 proteins were shared between the two groups (Figure 2c). The scatter plot of PSMs for these 618 proteins revealed 150 proteins with PSM values greater than 1.5 times that of the control group, indicating that curcumin protects these proteins from being hydrolyzed (Figure 2d). In total, 232 potential protein targets of curcumin were obtained through DARTS (82 binding proteins specific to the curcumin group were labeled yellow in Figure 2c, and 150 binding proteins in the

Table 1. Key Targets in Focal Adhesion

Uniprot ID	protein names	gene name	mol. weight [kDa]	score
A1BN54	alpha-actinin-1	Actn1	102.72	74.58
Q6NXW0	RAC-gamma serine/threonine-protein kinase	Akt3	55.66	18.42
P61750	ADP-ribosylation factor 4	Arf4	20.40	2.43
E9PYT0	rho GTPase-activating protein 5	Arhgap5	172.47	31.38
Q8R486	calpain-2 catalytic subunit	Capn2	48.33	17.49
Q542X7	T-complex protein 1 subunit beta	Cct2	57.48	100.89
Q8BPE7	uncharacterized protein (fragment)	Crk	28.42	2.19
Q3T9X3	dynamamin-2	Dnm2	97.19	16.48
G3UXY9	ectonucleotide phosphodiesterase family member 2	Enpp2	104.63	11.29
Q9QUP5	hyaluronan and proteoglycan link protein 1	Hapln1	40.45	21.45
P17156	heat shock-related 70 kDa protein 2	Hspa2	69.60	9.05
Q3TB63	uncharacterized protein (fragment)	Hspa8	50.43	19.30
F6RPJ9	insulin-degrading enzyme	Ide	114.15	42.53
P46660	alpha-internexin	Ina	55.38	18.53
P33175	kinesin heavy chain isoform 5A	Kif5a	117.02	11.71
Q80W81	mitogen-activated protein kinase	Mapk10	48.23	7.72
D3Z6D8	mitogen-activated protein kinase 3	Mapk3	30.60	2.47
Q05DD2	neurofilament light polypeptide	Nefl	57.83	12.02
F2Z3Z9	3-phosphoinositide-dependent protein kinase 1	Pdpk1	48.78	2.03
Q9JJV2-3	isoform 3 of profilin-2	Pfn2	9.80	3.64
A0JNZ1	phosphatidylinositol 4,5-bisphosphate 3-kinase catalytic subunit beta isoform	Pik3cb	119.64	6.97
Q6S390	plectin	Plec	506.45	29.95
O08586	phosphatidylinositol 3,4,5-trisphosphate 3-phosphatase and dual-specificity protein phosphatase PTEN	Pten	47.15	35.36
P63011	Ras-related protein Rab-3A	Rab3a	24.95	8.37
P67984	60S ribosomal protein L22	Rpl22	14.75	3.74
P99027	60S acidic ribosomal protein P2	Rplp2	11.64	2.28
Q9D1M0	protein SEC13 homologue	Sec13	35.54	4.39
Q3USK4	son of sevenless homologue 1	Sos1	129.23	11.40
Q8BYI9-2	isoform 2 of tenascin-R	Tnr	139.64	36.59
P68369	tubulin alpha-1A chain	Tuba1a	50.10	109.52
Q9CWF2	tubulin beta-2B chain	Tubb2b	49.92	90.24
Q9ERD7	tubulin beta-3 chain	Tubb3	50.39	63.37
Q9D6F9	tubulin beta-4A chain	Tubb4a	49.59	171.21

curcumin group whose PSM values were higher than those of the DMSO group were labeled yellow above the dashed line in Figure 2d).

Analysis of Key Pathways and Subcellular Localizations of Candidate Targets of Curcumin in Epileptic Mice. Given the many cellular targets of curcumin,^{15,16} we employed bioinformatics analysis to predict the key pathways in which it might be involved. Using the KEGG analysis tool, we screened the 70 candidate targets identified via affinity chromatography and the 232 candidate targets identified via DARTS and obtained 50 KEGG signaling pathways predicted to be associated with these targets. We selected the top 20 pathways for analysis with $p \leq 0.01$. KEGG enrichment results indicated an association of these targets with focal adhesion regulation (Figure 3a). Focal adhesion is a complex plasma membrane-related macromolecular assembly that includes integrin and multiprotein structures forming mechanical connections between intracellular actin bundles and the extracellular matrix (ECM).¹⁷ GO molecular function enrichment analysis suggested that these targets are related to a structural component of the cell skeleton (Figure 3b). In summary, the predictive results suggest that focal adhesion in the regulation of the cell skeleton is a key pathway that is influenced by curcumin and plays a critical role in the

progression of epilepsy. Protein targets from our screens that are related to focal adhesion are listed in Table 1.

In this study, a total of 302 different candidate targets from DARTS and affinity chromatography methods were obtained. The aim is to include a wider range of curcumin targets. Their subcellular localization indicated that 38.73% of the targets primarily localized in the cytoplasmic soluble fraction followed by the nucleus at 14.92% and the cytoskeleton at 11.75% (Figure 3c). The proportions of targets in the plasma membrane, synapses, Golgi apparatus, endoplasmic reticulum, mitochondria, and ECM were all below 10%. Other localizations, including axons, centrosomes, lysosomes, and ribosomes, accounted for 9.21%. Relative to other studies related to subcellular localization, cytoskeleton-related proteins appear to be relatively important in this study.^{18–20}

Functional Validation of Curcumin Candidate Pathway. PTN is a secreted cellular factor related to the ECM, and its expression levels are elevated in epileptic rats.²¹ PTN, as an important neuroregulator, plays various roles in the central nervous system, including neuronal survival, differentiation, and migration.²² Focal adhesion based cell ECM interactions are essential for cell anchoring and migration. To determine if curcumin regulates the focal adhesion pathway, we analyzed FAK localization and cell migration using U251 cells exposed to curcumin and then subjected to immunofluorescence

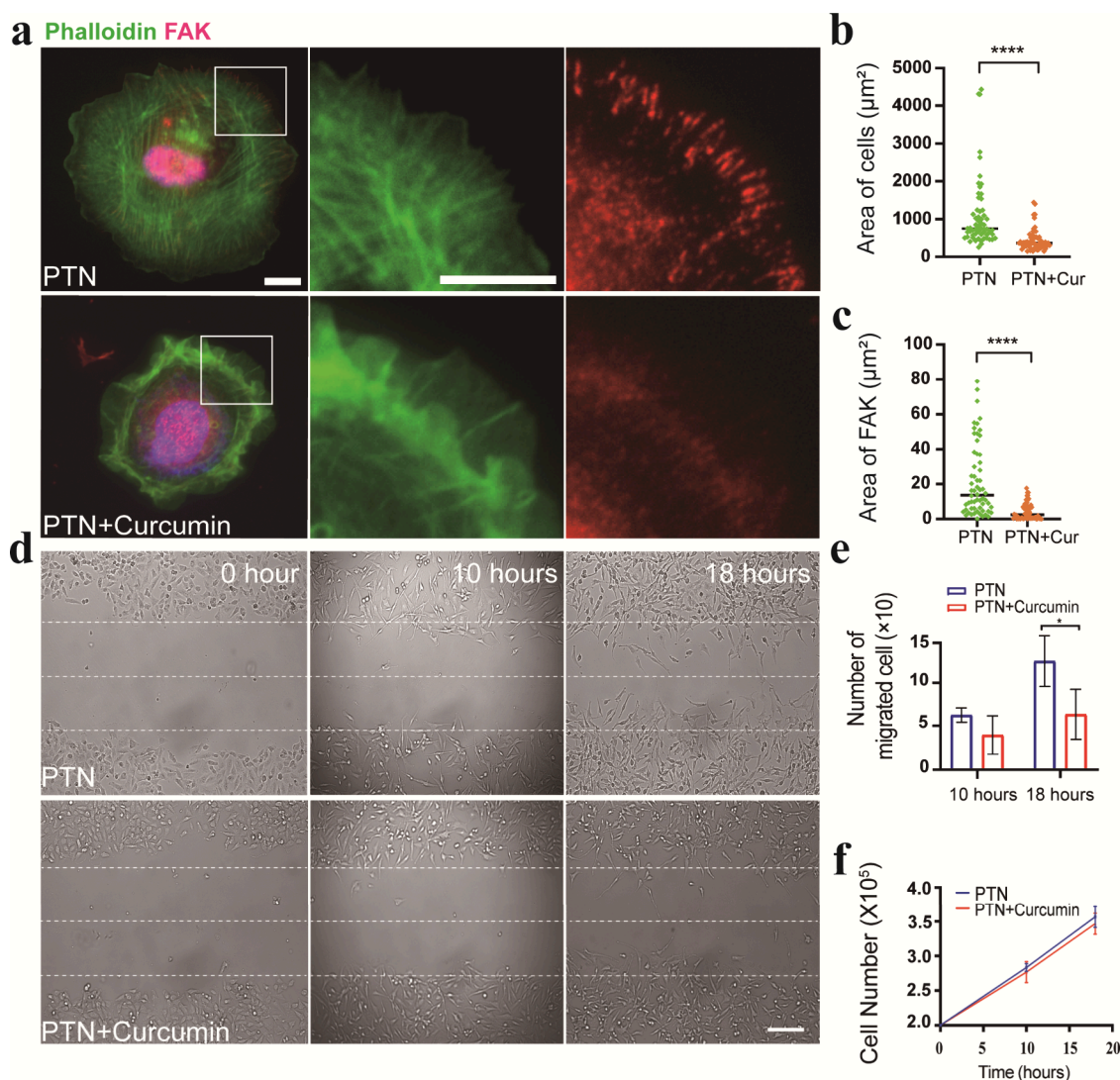


Figure 4. Curcumin affects cell migration via regulation of focal adhesion. (a) Immunofluorescent images showing control (PTN) and treated (PTN + curcumin) U251 cells subjected to staining to visualize phalloidin and FAK. Scale bars represent 10 and 30 μm . (b) Statistical analysis of area per cell in samples from panel a (Student's *t* test, values are means \pm SD, $n > 60$ for each group, $***P < 0.001$, significant difference compared with control/treated). (c) Statistical analysis of FAK area, i.e., the area of the cell with FAK signal, in samples from panel a (Student's *t* test, values are means \pm SD, $n > 60$ for each group, $***P < 0.001$, significant difference compared with control/treated). (d) Wound healing assay in control (PTN) and treated (PTN + curcumin) U251 cells demonstrating that cell invasion into the cell-free region is decelerated in curcumin-treated cells compared to control. The scale bar represents 200 μm . (e, f) Statistical charts of the number of migrated cells and total number of cells during the time course of the experiment (Student's *t* test, values are means \pm SD, $n = 3$ for each group, $**P < 0.01$, significant difference compared with control for 18 h).

microscopy. The experimental results showed that after curcumin with PTN administration, the area of u251 cells was reduced from 747.8 to 359.9 μm^2 , which was a significant reduction compared with the PTN group (Figure 4a,b). Moreover, after curcumin with PTN administration, the FAK area was reduced from 13.65 to 2.43 μm^2 . Therefore, curcumin can affect the distribution and localization of FAK at the cell edge (Figure 4a–c). In addition, the results of the wound healing experiment showed that curcumin with PTN for 10 h could be observed to slow down the migration rate of U251 cells, but there was no statistically significant difference compared with the PTN group. Compared with the curcumin with PTN group, the cell migration rate in the curcumin group slowed down significantly at 18 h; curcumin and PTN did not affect cell proliferation (Figure 4d–f).

Identification of Molecular Targets for Curcumin Using DARTS.

To identify the candidate targets for curcumin by DARTS, we use the intersection strategy. Seventy curcumin-binding targets were obtained by affinity chromatography, and 232 curcumin-binding targets were obtained by DARTS; the intersection of these two methods simultaneously revealed five common targets (Figure 5a). Considering that the DARTS sample strip by mass spectrometry is larger than 75 kDa (Figure 2b), among the five candidate targets, the molecular weight of choroideremia (CHM) and tubulin beta 4A (TUBB4A) was less than 75 kDa (Figure 5b), and only ubiquitin-specific proteases 5 (USP5), tenascin-R (TNR), and calcium-dependent secretion activators (CADPS) had molecular weights greater than 75 kDa, which fit our data requirements. Given that USP5 has been reported as a potential target for curcumin, we first selected it for validation.

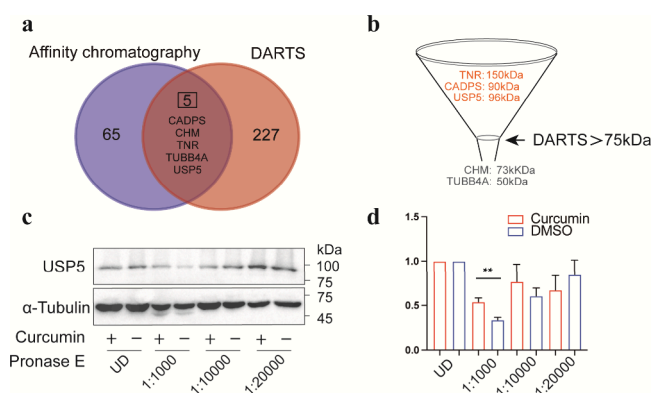


Figure 5. Identification of the target of curcumin. (a) A Venn diagram showing that only five protein targets, namely, CADPS, CHM, TNR, TUBB4A, and USP5, were found in both groups of proteins identified by DARTS and affinity chromatography methods. (b) Of the five candidate targets, only TNR, CADPS, and USP5 had molecular weights greater than 75 kDa consistent with the bands of interest in the analyzed DARTS samples (Figure 2b). (c) Western blotting analysis of USP5 in U251 cell extracts subjected to pronase E in the presence or absence of curcumin for verification of earlier DARTS results. (d) Quantitative analysis of the results from panel c showing that USP5 is protected from proteolysis in the presence of curcumin, implicating it as a verified target protein of curcumin. Data are mean \pm S.E.M., $n = 4$ biologically independent experiments by Student's t test ($P = 0.005$, $**P < 0.01$).

The results showed that with the increase of pronase E concentration, the ability of curcumin to protect USP5 increased, preventing USP5 from being hydrolyzed. When the ratio of pronase E to protein was 1:1000, it was statistically significant (Figure 5c,d).

DISCUSSION

Curcumin is a compound derived from turmeric, a plant that has been traditionally used to treat epilepsy.¹¹ Although curcumin has multiple targets, its exact mechanism for treating epilepsy is still not completely understood. We conducted a study using a combination of techniques to identify the molecular targets of curcumin. Our findings indicate that curcumin affects the cell migration and cytoskeleton through potential targets such as USP5, TNR, and CADPS. These results suggest that these factors may play an important role in treating epilepsy.

Cytoskeleton and Cell Migration Are Important Factors in the Pathogenesis of Epilepsy. Epilepsy is a complex neurological disorder characterized by recurrent seizures and involves complex cellular processes in the brain, in which the role of the cytoskeleton and cell migration is crucial.²³

The cytoskeleton includes actin filaments, microtubules, and intermediate filaments. These basic cellular structures are crucial not only for maintaining cell shape but also for the complex processes of cellular transport, division, and cell migration.²⁴ Cell migration, especially during brain development, is critical for the correct positioning of neurons.²⁵ This process relies heavily on the cytoskeleton, which facilitates cell movement to predetermined positions in the cerebral cortex.²⁶ Abnormalities in cytoskeletal dynamics may lead to inappropriate neuronal migration, leading to conditions such as anencephaly, a condition associated with severe epilepsy due to structural disruption of the brain.²⁷ Furthermore, the

importance of the cytoskeleton extends to astrocytes, which undergo changes in shape and mobility in response to brain injury, leading to the formation of glial scars.²⁸ These scars can alter neuronal connections and exacerbate the conditions that trigger seizures.²⁹ The cytoskeleton also plays a key role in maintaining the structure of the blood–brain barrier (BBB) and neuronal dendrites and spines, influencing synaptic function and plasticity, both of which are critical in the development of epilepsy.^{30,31} Our study suggests that curcumin may play a role by regulating the cytoskeleton and cell movement. This finding is consistent with the current understanding of brain development and the pathogenesis of epilepsy. Our study not only provides insights into the underlying mechanisms of the disease but also provides an example of research methods for related clinical studies.

USP5, TNR, and CADPS Impacts in the Cytoskeleton and Cell Migration. We used the DARTS method combined with affinity chromatography to identify the targets of curcumin. The results showed that curcumin can regulate cell movement through USP5, TNR, and CADPS.

USP5 is an enzyme that belongs to the USP family and plays a crucial role in cysteine deubiquitination.³² Research shows that USP5 regulates EMT, which affects cell movement via the Wnt/ β -catenin signaling pathway and mTOR/4EBP1 pathway.³³ TNR is a glycoprotein exclusively found in the central nervous system. It belongs to the tenascin family of ECM glycoproteins.³⁴ TNR promotes neuronal process growth, induces neuronal morphology polarization, and is related to myelin formation.³⁵ KEGG pathway analysis revealed that TNR is a crucial component of ECM glycoproteins, and it regulates cell migration by controlling FAK phosphorylation; CADPS has two isoforms, CAPS1 and CAPS2, and is involved in the exocytosis of synapses and DCVs in neurons and neuroendocrine cells.³⁶ Studies have shown that CAPS1 regulates cell migration by controlling the secretion of exosomes.³⁷ CAPS1 also promotes colorectal cancer metastasis through the epithelial–mesenchymal transition process mediated by the PI3K/Akt signaling pathway.³⁸

Our experimental results suggest that curcumin has a significant regulatory effect on cell motility, which may be due to USP5, TNR, and CADPS. We have used the DARTS method combined with affinity chromatography to demonstrate this combination of methods. We will carry out additional research to gain a more thorough understanding of its molecular mechanism.

The Advantages and DARTS Combined with Affinity Chromatography. Determining the targets is a crucial step in establishing the correlation between chemical components and pharmacological effects. However, traditional target screening methods have limitations due to the diversity of Chinese medicine, formulations, and complexity of chemical components. This has made target identification a bottleneck in the research of the mechanism of action of Chinese medicine.

Affinity chromatography is a commonly used technique to identify targets by modifying small molecules and attaching them to sepharose EAS6B as a stationary phase for screening and enrichment of target proteins.³⁹ Although this method has been successful, it requires chemical modification, which may alter the activity of the drugs. On the other hand, DARTS is a newer technology in chemical proteomics that allows the identification and screening of complex chemical components without modifying their native activity.⁴⁰ The method directly confers resistance to protease hydrolysis on target proteins,

making it proteome-based and relatively fast for identifying potential protein targets of small molecules. However, the DARTS method has some limitations. The differential bands sent for inspection using mass spectrometry are limited, and only specific target points within a certain molecular weight range can be obtained.

Our study has found that using a combination of biotechnologies is beneficial in identifying small molecule targets. This approach can produce more reliable results and provide direction for future research. However, we have obtained a relatively small number of target proteins in our experiments, and the sensitivity needs improvement. Furthermore, the outcomes need validation and support from a significant amount of biological research.

CONCLUSIONS

Through our research, we have demonstrated an experimental system that combines DARTS and affinity chromatography. This system aims to identify potential targets for curcumin, a promising treatment for epilepsy. Our findings have revealed that USPS, CADPS, and TNFR are the potential target proteins for curcumin. These proteins play a critical role in regulating physiological processes such as the cytoskeleton and cell movement, which are closely associated with brain development and pathological processes like epilepsy.

Our research has demonstrated that the combination of DARTS and affinity chromatography is a promising technique for identifying small molecule targets. This approach can be helpful in the quest for targets for disease treatment and can also aid in comprehending the mechanism of action of complex drug ingredients.

ASSOCIATED CONTENT

Supporting Information

The Supporting Information is available free of charge at <https://pubs.acs.org/doi/10.1021/acsomega.4c00825>

DARTS using brain lysate subjected to CBB staining (Figure S1) (PDF)

AUTHOR INFORMATION

Corresponding Author

Qi Xie – *Wangjing Hospital of China Academy of Chinese Medical Sciences, Beijing 100102, China*; Phone: 86-10-84739188; Email: xieqixieqi@139.com; Fax: 86-10-84739188

Authors

Ninan Zhang – *Institute of Acupuncture and Moxibustion, China Academy of Chinese Medical Sciences, Beijing 100700, China*; *Institute of Basic Research in Clinical Medicine, China Academy of Chinese Medical Sciences, Beijing 100700, China*; *State Key Laboratory of Molecular Developmental Biology, Institute of Genetics and Developmental Biology, Chinese Academy of Sciences, Beijing 10019, China*

Ruifan Lin – *Institute of Basic Research in Clinical Medicine, China Academy of Chinese Medical Sciences, Beijing 100700, China*; *State Key Laboratory of Molecular Developmental Biology, Institute of Genetics and Developmental Biology, Chinese Academy of Sciences, Beijing 10019, China*;
orcid.org/0009-0006-7727-8088

Honglin Xu – *State Key Laboratory of Molecular Developmental Biology, Institute of Genetics and*

Developmental Biology, Chinese Academy of Sciences, Beijing 10019, China

Xianghong Jing – *Institute of Acupuncture and Moxibustion, China Academy of Chinese Medical Sciences, Beijing 100700, China*

Hongwei Zhou – *National Data Center of Traditional Chinese Medicine, China Academy of Chinese Medical Sciences, Beijing 100700, China*

Xiaoxiao Wen – *National Data Center of Traditional Chinese Medicine, China Academy of Chinese Medical Sciences, Beijing 100700, China*

Complete contact information is available at:

<https://pubs.acs.org/10.1021/acsomega.4c00825>

Author Contributions

#N.Z. and R.L. contributed equally to this work.

Author Contributions

N.Z., R.L., and Q.X. designed all experiments, interpreted the results, and prepared the manuscript. H.X., H.Z., X.W., and X.J. provided advice.

Notes

The authors declare no competing financial interest.

ACKNOWLEDGMENTS

This work was supported by the China Academy of Chinese Medical Sciences (CACMS), the Innovation Fund (C12021A05023), and the Beijing of Chinese Medicine Science and Technology Development Fund (JJ-2020-68). Special thanks to Professor Wenxiang Meng from the Institute of Genetic and Developmental Biology for his guidance on this paper. We are grateful to Tao Jiang for advice. Thanks to Dr. Han Ding from the Capital Normal University for his exquisite traditional Chinese painting of *Curcuma longa* featured on our magazine cover. Thanks to the "<https://depositphotos.com/cn/home.html>" website for providing the pictures used in the abstract graphics, which are numbered 243936862, 248983544, and 323080318.

REFERENCES

- (1) Fisher, R. S.; Acevedo, C.; Arzimanoglou, A.; Bogacz, A.; Cross, J. H.; Elger, C. E.; Engel, J.; Forsgren, L.; French, J. A.; Glynn, M.; et al. ILAE official report: a practical clinical definition of epilepsy. *Epilepsia* **2014**, *55* (4), 475–482.
- (2) Kwan, P.; Arzimanoglou, A.; Berg, A. T.; Brodie, M. J.; Allen Hauser, W.; Mathern, G.; Moshé, S. L.; Perucca, E.; Wiebe, S.; French, J. Definition of drug resistant epilepsy: consensus proposal by the ad hoc Task Force of the ILAE Commission on Therapeutic Strategies. *Epilepsia* **2010**, *51* (6), 1069–1077.
- (3) Schuele, S. U.; Lüders, H. O. Intractable epilepsy: management and therapeutic alternatives. *Lancet Neurol.* **2008**, *7* (6), 514–524.
- (4) Nelson, K. M.; Dahlin, J. L.; Bissson, J.; Graham, J.; Pauli, G. F.; Walters, M. A. The Essential Medicinal Chemistry of Curcumin. *J. Med. Chem.* **2017**, *60* (5), 1620–1637.
- (5) Gupta, S. C.; Kismali, G.; Aggarwal, B. B. Curcumin, a component of turmeric: from farm to pharmacy. *Biofactors* **2013**, *39* (1), 2–13.
- (6) Morawski, M.; Dityatev, A.; Hartlage-Rubsamen, M.; Blosa, M.; Holzer, M.; Flach, K.; Pavlica, S.; Dityateva, G.; Grosche, J.; Brückner, G.; et al. Tenascin-R promotes assembly of the extracellular matrix of perineuronal nets via clustering of aggrecan. *Philos. Trans R Soc. Lond B Biol. Sci.* **2014**, *369* (1654), 20140046.
- (7) Simian, D.; Fluxa, D.; Flores, L.; Lubascher, J.; Ibanez, P.; Figueroa, C.; Kronberg, U.; Acuña, R.; Moreno, M.; Quera, R.

- Inflammatory bowel disease: A descriptive study of 716 local Chilean patients. *World J. Gastroenterol* **2016**, *22* (22), 5267–5275.
- (8) Reeta, K. H.; Mehla, J.; Pahuja, M.; Gupta, Y. K. Pharmacokinetic and pharmacodynamic interactions of valproate, phenytoin, phenobarbitone and carbamazepine with curcumin in experimental models of epilepsy in rats. *Pharmacol., Biochem. Behav.* **2011**, *99* (3), 399–407.
- (9) Mirza, N.; Sills, G. J.; Pirmohamed, M.; Marson, A. G. Identifying new antiepileptic drugs through genomics-based drug repurposing. *Hum. Mol. Genet.* **2017**, *26* (3), ddd410–537.
- (10) Pai, M. Y.; Lomenick, B.; Hwang, H.; Schiestl, R.; McBride, W.; Loo, J. A.; Huang, J. Drug affinity responsive target stability (DARTS) for small-molecule target identification. *Methods Mol. Biol.* **2015**, *1263*, 287–298.
- (11) Dhir, A. Curcumin in epilepsy disorders. *Phytother Res.* **2018**, *32* (10), 1865–1875.
- (12) TurSKI, L.; Ikonomidou, C.; TurSKI, W. A.; Bortolotto, Z. A.; Cavalleiro, E. A. Review: cholinergic mechanisms and epileptogenesis. The seizures induced by pilocarpine: a novel experimental model of intractable epilepsy. *Synapse* **1989**, *3* (2), 154–171.
- (13) TurSKI, W. A.; Cavalleiro, E. A.; Schwarz, M.; Czuczwar, S. J.; Kleinrok, Z.; TurSKI, L. Limbic seizures produced by pilocarpine in rats: behavioural, electroencephalographic and neuropathological study. *Behav Brain Res.* **1983**, *9* (3), 315–335.
- (14) Racine, R. J. Modification of seizure activity by electrical stimulation. II. Motor seizure. *Electroencephalogr Clin Neurophysiol* **1972**, *32* (3), 281–294.
- (15) Kunnumakkara, A. B.; Bordoloi, D.; Padmavathi, G.; Monisha, J.; Roy, N. K.; Prasad, S.; Aggarwal, B. B. Curcumin, the golden nutraceutical: multitargeting for multiple chronic diseases. *Br. J. Pharmacol.* **2017**, *174* (11), 1325–1348.
- (16) Pourbagher-Shahri, A. M.; Farkhondeh, T.; Ashrafzadeh, M.; Talebi, M.; Samarghandian, S. Curcumin and cardiovascular diseases: Focus on cellular targets and cascades. *Biomed Pharmacother* **2021**, *136*, No. 111214.
- (17) Abercrombie, M.; Dunn, G. A. Adhesions of fibroblasts to substratum during contact inhibition observed by interference reflection microscopy. *Exp. Cell Res.* **1975**, *92* (1), 57–62.
- (18) Liu, Y.; Lan, X.; Song, S.; Yin, L.; Dry, I. B.; Qu, J.; Xiang, J.; Lu, J. In Planta Functional Analysis and Subcellular Localization of the Oomycete Pathogen *Plasmopara viticola* Candidate RXLR Effector Repertoire. *Front Plant Sci.* **2018**, *9*, 286.
- (19) Loo, L. H.; Laksameethanasan, D.; Tung, Y. L. Quantitative Protein Localization Signatures Reveal an Association between Spatial and Functional Divergences of Proteins. *Plos Computational Biology* **2014**, *10*(3).
- (20) Zhang, H.; Cao, X.; Tang, M.; Zhong, G.; Si, Y.; Li, H.; Zhu, F.; Liao, Q.; Li, L.; Zhao, J.; Feng, J.; Li, S.; Wang, C.; Kaulich, M.; Wang, F.; Chen, L.; Li, L.; Xia, Z.; Liang, T.; Lu, H.; Feng, X. H.; Zhao, B.; et al. A subcellular map of the human kinome. *Elife* **2021**, *10*.
- (21) Zhang, S.; Liang, F.; Wang, B.; Le, Y.; Wang, H. Elevated expression of pleiotrophin in pilocarpine-induced seizures of immature rats and in pentylene-tetrazole-induced hippocampal astrocytes in vitro. *Acta Histochem* **2014**, *116* (2), 415–420.
- (22) Asai, H.; Morita, S.; Miyata, S. Effect of pleiotrophin on glutamate-induced neurotoxicity in cultured hippocampal neurons. *Cell Biochem Funct* **2011**, *29* (8), 660–665.
- (23) Stouffer, M. A.; Golden, J. A.; Francis, F. Neuronal migration disorders: Focus on the cytoskeleton and epilepsy. *Neurobiol Dis* **2016**, *92* (Pt A), 18–45.
- (24) Hohmann, T.; Dehghani, F. The Cytoskeleton-A Complex Interacting Meshwork. *Cells* **2019**, *8*, 362.
- (25) Marin, O.; Valiente, M.; Ge, X.; Tsai, L. H. Guiding neuronal cell migrations. *Cold Spring Harb Perspect Biol.* **2010**, *2* (2), a001834.
- (26) Javier-Torrent, M.; Zimmer-Bensch, G.; Nguyen, L. Mechanical Forces Orchestrate Brain Development. *Trends Neurosci* **2021**, *44* (2), 110–121.
- (27) Gambino, G.; Rizzo, V.; Giglia, G.; Ferraro, G.; Sardo, P. Microtubule Dynamics and Neuronal Excitability: Advances on Cytoskeletal Components Implicated in Epileptic Phenomena. *Cell Mol. Neurobiol* **2022**, *42* (3), 533–543.
- (28) Schiweck, J.; Eickholt, B. J.; Murk, K. Important Shapeshifter: Mechanisms Allowing Astrocytes to Respond to the Changing Nervous System During Development, Injury and Disease. *Front. Cell Neurosci.* **2018**, *12*, 261.
- (29) Robel, S. Astroglial Scarring and Seizures: A Cell Biological Perspective on Epilepsy. *Neuroscientist* **2017**, *23* (2), 152–168.
- (30) Pottiez, G.; Sevin, E.; Cecchelli, R.; Karamanos, Y.; Flahaut, C. Actin, gelsolin and filamin-A are dynamic actors in the cytoskeleton remodelling contributing to the blood brain barrier phenotype. *Proteomics* **2009**, *9* (5), 1207–1219.
- (31) Witte, H.; Bradke, F. The role of the cytoskeleton during neuronal polarization. *Curr. Opin Neurobiol* **2008**, *18* (5), 479–487.
- (32) Ning, F.; Xin, H.; Liu, J.; Lv, C.; Xu, X.; Wang, M.; Wang, Y.; Zhang, W.; Zhang, X. Structure and function of USP5: Insight into physiological and pathophysiological. *Pharmacol. Res.* **2020**, *157*, No. 104557.
- (33) Li, Y.; Zhou, J. USP5 Promotes Uterine Corpus Endometrial Carcinoma Cell Growth and Migration via mTOR/4EBP1 Activation. *Cancer Manag Res.* **2021**, *13*, 3913–3924.
- (34) Anlar, B.; Gunel-Ozcan, A. Tenascin-R: role in the central nervous system. *Int. J. Biochem. Cell Biol.* **2012**, *44* (9), 1385–1389.
- (35) Jakovcevski, I.; Miljkovic, D.; Schachner, M.; Andjus, P. R. Tenascins and inflammation in disorders of the nervous system. *Amino Acids* **2013**, *44* (4), 1115–1127.
- (36) Shaib, A. H.; Staudt, A.; Harb, A.; Klose, M.; Shaaban, A.; Schirra, C.; Mohrmann, R.; Rettig, J.; Becherer, U. Paralogs of the Calcium-Dependent Activator Protein for Secretion Differentially Regulate Synaptic Transmission and Peptide Secretion in Sensory Neurons. *Front. Cell Neurosci.* **2018**, *12*, 304.
- (37) Wu, B.; Sun, D.; Ma, L.; Deng, Y.; Zhang, S.; Dong, L.; Chen, S. Exosomes isolated from CAPS1-overexpressing colorectal cancer cells promote cell migration. *Oncol. Rep.* **2019**, *42* (6), 2528–2536.
- (38) Zhao, G. X.; Xu, Y. Y.; Weng, S. Q.; Zhang, S.; Chen, Y.; Shen, X. Z.; Dong, L.; Chen, S. CAPS1 promotes colorectal cancer metastasis via Snail mediated epithelial mesenchymal transformation. *Oncogene* **2019**, *38* (23), 4574–4589.
- (39) Firouzi, Z.; Lari, P.; Rashedinia, M.; Ramezani, M.; Iranshahi, M.; Abnous, K. Proteomics screening of molecular targets of curcumin in mouse brain. *Life Sciences* **2014**, *98* (1), 12–17.
- (40) Lomenick, B.; Jung, G.; Wohlschlegel, J. A.; Huang, J. Target identification using drug affinity responsive target stability (DARTS). *Curr. Protoc Chem. Biol.* **2011**, *3* (4), 163–180.